

Detection of Ionizing Radiation Using Graphene Field Effect Transistors

Michael Foxe*, *Student Member, IEEE*, Gabriel Lopez*, *Student Member, IEEE*, Isaac Childres, Romaneh Jalilian, Caleb Roecker, John Boguski, Igor Jovanovic#, and Yong P. Chen#, *Member, IEEE*

Abstract– The use of graphene field effect transistors (GFET) to detect ionizing radiation is proposed. The detection mechanism used in the proposed detector architectures is based on the high sensitivity of graphene to the local change of electric field that can result from the interaction of radiation with a semiconductor substrate in a GFET. We present preliminary modeling work to develop a prototype graphene-based radiation detector (GRD), and discuss its potential advantages compared to conventional detector architectures.

I. INTRODUCTION

HIGH-PERFORMANCE sensors for penetrating ionizing radiation (γ -rays and neutrons) are important for many scientific and commercial applications. For example, sensors are needed in nuclear security to facilitate detection of special nuclear materials (SNM) with high signal-to-noise ratios. A major challenge in the development of radiation sensors, particularly those for γ -rays, is achieving high energy resolution at room temperature. We are exploring the exceptional electronic properties of graphene (a single atomic layer of graphite) [1] to develop graphene-based devices with a potential to improve the performance of radiation sensors.

Manuscript received February 5, 2010. This work has been funded by National Science Foundation, Department of Homeland Security, and Department of Defense under awards 0833689-ECCS, 2009-DN-077-ARI036-02, and HDTRA1-09-1-0047 respectively

*: M. Foxe and G. Lopez made equal contributions to this paper.

#: Correspondence should be addressed to I. Jovanovic and Y. P. Chen.

M. Foxe is with the School of Nuclear Engineering, Purdue University, West Lafayette, IN 47907 USA (e-mail: mfoxe@purdue.edu).

G. Lopez is with the School of Electrical Engineering, Purdue University, West Lafayette, IN 47907 USA and with Birck Nanotechnology Center, Purdue University, West Lafayette, IN 47907 USA (e-mail: glopez@ecn.purdue.edu).

I. Childres is with the Department of Physics, Purdue University, West Lafayette, IN 47907 USA and with Birck Nanotechnology Center, Purdue University, West Lafayette, IN 47907 USA (e-mail: almagest@purdue.edu).

R. Jalilian is with the Department of Physics, Purdue University, West Lafayette, IN 47907 USA and with Birck Nanotechnology Center, Purdue University, West Lafayette, IN 47907 USA (e-mail: rjalilia@purdue.edu).

C. Roecker is with the School of Nuclear Engineering, Purdue University, West Lafayette, IN 47907 USA (e-mail: croecker@purdue.edu).

J. Boguski is with the School of Nuclear Engineering, Purdue University, West Lafayette, IN 47907 USA (e-mail: jboguski@purdue.edu).

I. Jovanovic is with the School of Nuclear Engineering, Purdue University, West Lafayette, IN 47907 USA (e-mail: ijovanovic@purdue.edu).

Y.P. Chen is with the Department of Physics, Purdue University, West Lafayette, IN 47907 USA, with the School of Electrical Engineering, Purdue University, West Lafayette, IN 47907 USA and with Birck Nanotechnology Center, Purdue University, West Lafayette, IN 47907 USA (e-mail: yongchen@purdue.edu).

Here we present the principles of operation and the results of our modeling work on graphene-based radiation detectors. Our prototype device architecture is a graphene field-effect transistor (GFET) [2], consisting of graphene on a radiation-absorbing, electrically gated undoped semiconductor substrate, separated from graphene by a thin dielectric buffer layer. The technical approach is to utilize the sensitive dependence of the electrical conductivity of graphene on a local electric field, which can be abruptly changed by charge carriers produced by ionizing radiation in the underlying absorber material. This dependence is sharp even at room temperature, which provides a unique opportunity to deploy graphene in conjunction with narrow-bandgap absorbers (such as InSb) with relaxed temperature, purity, carrier mobility, and lifetime constraints.

Using Monte Carlo simulations (MCNP-Polimi [3]), the interactions of both γ -rays and fast neutrons with various absorber materials (such as Si, Ge, and InSb) were modeled. The energy deposited and location of energy deposition was calculated in configurations resembling our prototype device. In the following discussion we focus on the detection of γ -rays. For the dominant mode of first interaction (Compton scattering), transport of energetic Compton electrons in the absorber was subsequently modeled using CASINO Monte Carlo code [4]. The calculated ionized charge distribution was used as an input into a COMSOL Multiphysics model [5] to calculate the change in electric field, which results in the modulation of conductivity of graphene.

II. GRAPHENE FIELD EFFECT TRANSISTORS

Graphene is a monolayer of graphite with unique electronic properties [1]. Graphene has a high carrier mobility, about 10 times the carrier mobility of Si at room temperature or better [2]. Graphene is a low noise electronic material and has a resistance which is very sensitive to local change of carrier density near the charge neutrality point (CNP) (Fig. 1), or “Dirac point” [6]. This feature has been exploited to detect the adsorption/desorption of a single molecule on graphene [6]. The sensitivity of resistance to charge carriers near the Dirac point allows for graphene to sense small changes in the electric field (Fig. 1) and is proposed to be exploited to sense ionizing radiation. This detection mechanism is analogous to utilizing the sharp feature of the superconductivity transition in a transition edge sensor (TES) [7].

In our prototype device, a GFET is coupled to a semiconductor radiation absorber through an insulating buffer

layer (Fig. 2). An electric field is produced by applying a gate voltage to the back of the absorber. There are four electrodes on the graphene for accurate 4-terminal resistance measurements, while 2-terminal measurements could be employed in the sensor in many practical situations. The drain and source electrodes supply the current through the graphene and are used to measure the voltage drop across the graphene. The local electric field at graphene determines its resistance via the field effect with the change in resistance being most sensitive to the local electric field when the graphene is near its “Dirac point” (Fig. 1) [2,6].

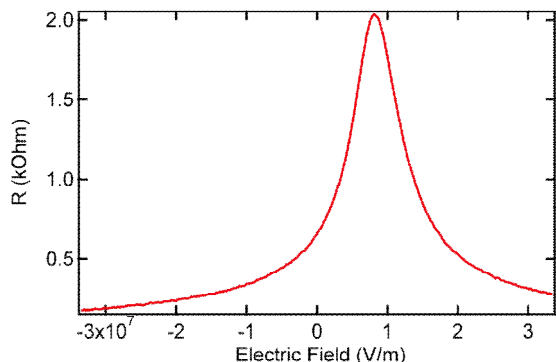


Fig. 1. Graphene exhibits a sharp peak (“Dirac point”) in resistance as a function of the electric field. Data shown are measured in a representative GFET (Fig. 2, with doped Si as substrate and 300nm-thick SiO₂ as buffer layer) at room temperature.

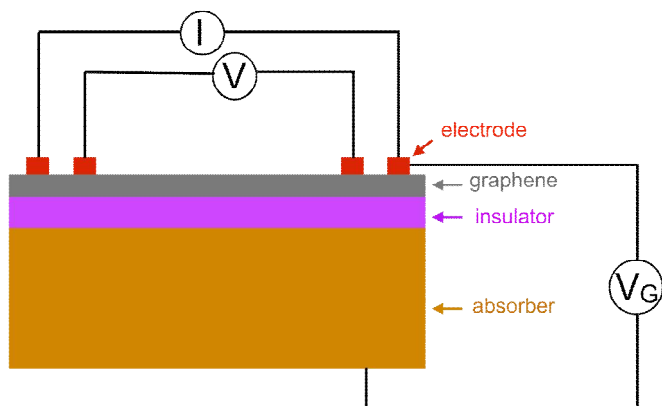


Fig. 2. A GFET consists of an absorber (semiconductor), with an insulating buffer layer which serves as a gate dielectric. V_G is the gate voltage applied to the sample. Current is supplied across the graphene sample, and the voltage is measured to obtain the resistance of the graphene layer.

III. DETECTING THE PRESENCE OF RADIATION WITHOUT DRIFTING THE CHARGES

A. Principle of operation: Ionization-Induced Change of the Electric Field

In a simplest scheme of using a GFET to detect radiation, the electric field at graphene can be abruptly altered by the change of the resistivity of the absorber upon interaction with ionizing radiation. Using an undoped, high resistivity

semiconductor as the absorber, the gate voltage drops across both the absorber and the buffer layer (Fig. 3). With a conductive absorber, the gate voltage drops primarily across the buffer layer, resulting in an increased electric field (Fig. 4).

Radiation interacting with the absorber results in ionization, which can increase the conductivity of the absorber, resulting in an electric field increase across the buffer layer (Fig. 4). The change in electric field is indirectly sensed by measuring the resistance of graphene. This transient change in resistance could be used to detect the presence of radiation interacting with the absorber, and the magnitude of resistance change is related to both the total energy (ionized charges) deposited into the absorber and the location of the ionized charges (Sec. III. C).

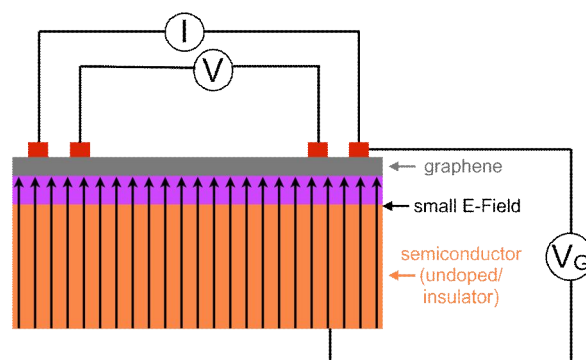


Fig. 3. When the undoped absorber acts as an insulator, the gate voltage (V_G) drops across both the absorber and the insulator, resulting in a relatively small electric field.

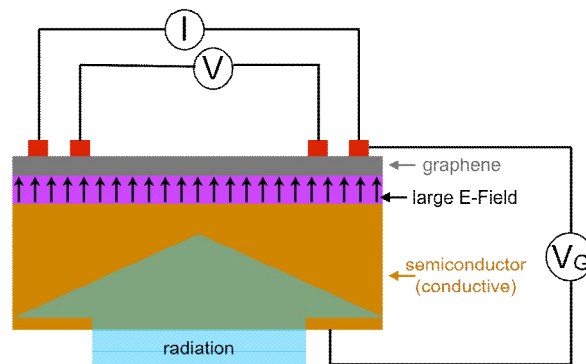


Fig. 4. The incoming radiation ionizes the intrinsic semiconductor to create a conducting absorber. The gate voltage (V_G) is now effectively “transferred” through the absorber and drops across the insulator. This results in an increased electric field which is detected by graphene via the field effect (Fig. 1) and is signaled by a corresponding change in resistance.

B. Monte Carlo Model for Radiation Interaction

The most commonly fabricated GFETs employ silicon wafers (typically covered by 300nm-thick SiO₂) as substrates [2]. Using MCNP-PoliMi [3], we modeled a Si-based GFET irradiated with a 1 MeV isotropic γ -ray source located 1 cm from the bottom of the absorber. The energy deposited and the position of interaction were calculated in the simulation. From the energy deposited, we modeled the electron

trajectories within the Si absorber using the monte CARLO SIMulation of electroN trajectory in sOLids (CASINO) code [4]. CASINO simulation shows a wide variation in electron trajectory characteristic for electron stopping (Fig. 7).

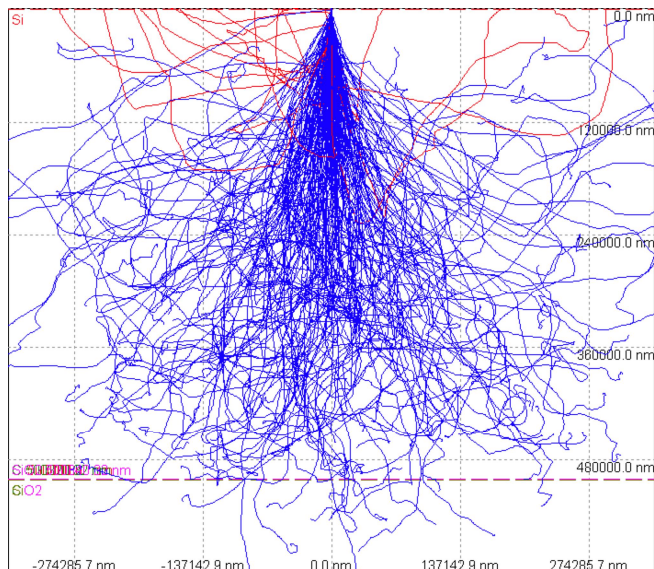


Fig. 7. A CASINO simulation of a beam of 400 keV electrons being emitted normal to a silicon wafer of 500 μm . The red tracks are the electrons which have been backscattered out of the absorber.

As a simple approximation, we split each electron track into two ionization regions with constant specific ionizations. The first ionization region represents the beginning of the electron track, while the second ionization region represents the vicinity of the Bragg peak, with a peak-to-tail specific ionization ratio calculated from CASINO. The CASINO simulations show a significant fraction of electrons escaping the Si absorber of standard wafer thickness (500 μm) once they reached energies above ~ 400 keV. For an electron energy of 400 keV, the number of electron-hole pairs created per unit distance within the absorber, (Fig. 8), is calculated using the Si W-value of 3.65 eV [8].

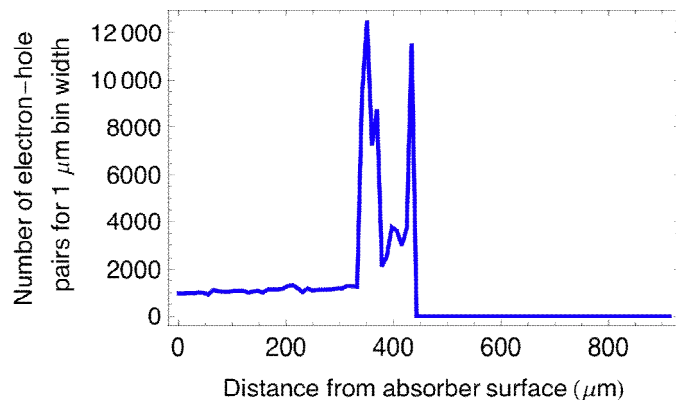


Fig. 8. Electron-hole pairs created per 1 μm for a 400 keV primary electron in a Si absorber using a 3.65 eV W-value.

C. COMSOL Model for Electronic Response

In conjunction with the MCNP modeling, finite element method (FEM) simulations were conducted in order to estimate the electric field distribution in a simplified model of the proposed GRD. The FEM platform utilized in the simulations was COMSOL Multiphysics 3.5a in the “conductive media DC” application mode for two dimensions. Poisson’s equation was solved in the model:

$$-\nabla \cdot (\sigma \nabla V - J^e) = Q_j, \quad (1)$$

where σ is conductivity, V is voltage, J^e is external current density, and Q_j is a current source. For simplicity and without loss of the important physics, the conductivity values for SiO_2 and the idealized highly insulating intrinsic Si substrate were taken to be 1×10^{-14} S/m in the model. Since the J^e and Q_j parameters were zero in the simulations, Poisson’s equation was reduced to Laplace’s equation.

The simplified device model consisted of a square-shaped highly insulating intrinsic Si substrate, measuring 500 μm by 500 μm , with a rectangular SiO_2 buffer layer, measuring 500 μm by 300 nm. The back gate of the GFET structure was located on the bottom of the Si substrate, while the graphene region was modeled as a grounded portion of the top surface of SiO_2 layer. Boundaries at the left and right border of the model were designated as insulating boundary conditions while the interior boundaries were maintained as continuity conditions. A triangular mesh of approximately 2×10^4 elements was generated for the simulations.

The simulation investigated the modulation of the electric field due to the generation of charges in the intrinsic Si substrate following an ionizing event. Carrier concentration data generated by MCNP simulations were used to determine the conductivity of the ionized regions in the model. The conductivities of ionization regions are much greater than those of the surrounding media (undoped Si or SiO_2). The model assumed that the back gate was biased at 10 V. Fig. 9 illustrates the effect of ionization regions on the distribution of the equipotential lines in the Si absorber for two different energy deposition profiles.

The results from the FEM simulations suggest that, in principle, an ionizing event is able to modulate the electric field in such a way as to produce a substantial change in the resistance of a nearby GFET. In the simulation, the *change* of electric field strength in the SiO_2 immediately above the ionized absorber region can be on the order of 10^6 - 10^7 V/m. An electric field change as large as that suggested by the simulation is capable of modulating the number carriers in graphene and produce a measurable change of resistance (Fig. 1). Also using COMSOL (FEM) simulation, we have illustrated that a grounded graphene region can serve to “funnel” charge carriers in the ionized absorber towards the Si- SiO_2 interface under a large back gate’s bias (Fig. 5), as we discuss in the next section.

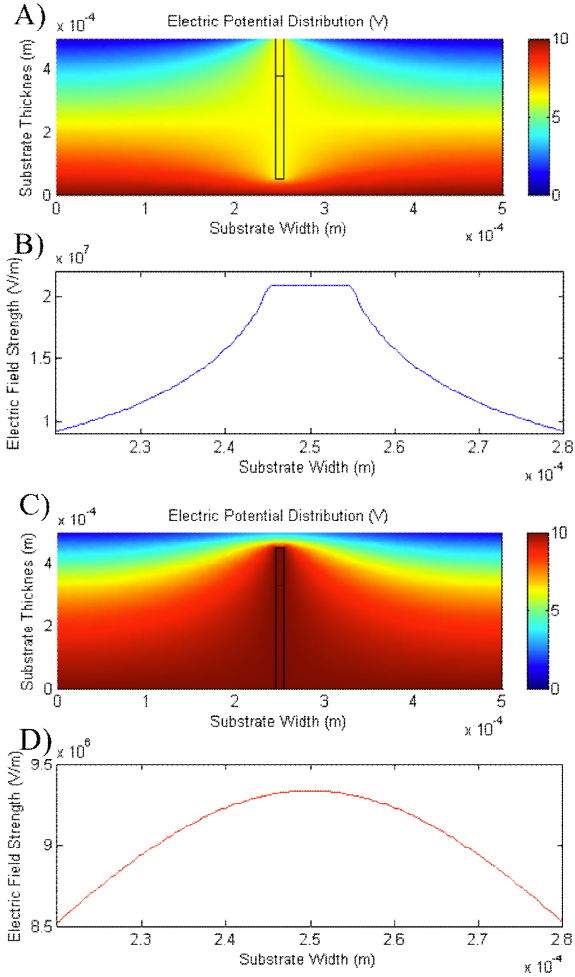


Fig. 9. Calculated distribution of the equipotential lines (A,C) and electric field profile (B, D) 1 nm into the SiO₂ top surface (near graphene) for two examples of ionization regions: one that reaches the Si/SiO₂ interface (A, B) and one that starts from the back gate boundary (C, D). The model assumed that the back gate biased at 10 V. The shape and profile of the ionization region (width=10 μ m) were selected for convenience of simulation and for demonstration purpose. Realistic ionization tracks would have more complicated profiles (Figs. 7, 8).

IV. DETECTION WITH ENERGY RESOLUTION: DRIFTING CHARGES

A. Principle of Operation

While the simple scheme described above could be used to detect the *presence* of ionizing radiation, in many applications such as SNM detection it is paramount to accurately measure the energy of the radiation deposited in the absorber. In such single-event radiation sensing, the absorber is ionized nonuniformly, and the morphology of charge deposition is highly random (Sec. III, Figs 7, 8). As a result, the electric field change near graphene has a poor correlation with the energy deposited in the substrate, which would compromise the ability to measure deposited energy through change of resistance. This issue can be addressed by

drifting the charge to the surface of the absorber, effectively normalizing the position of each interaction to the layer with a constant distance from graphene. This drift can be accomplished by the electric field applied between the electroically biased back gate electrode (at the back of absorber) and the top electrode (graphene). In a typical configuration, the back surface gate electrode is much larger than the graphene (top surface) electrode, creating curved electric field lines which become denser close to the graphene (Fig. 5 shows a COMSOL [4] simulation). The field lines “funnel” electrons created by the ionizing radiation in the absorber to the location directly under the graphene, resulting in an electric field response independent of where these ionized charges are originally produced in the absorber. Net change of electric field applied to graphene is now dependent only on the amount of charge, effectively correlating it with the energy deposited.

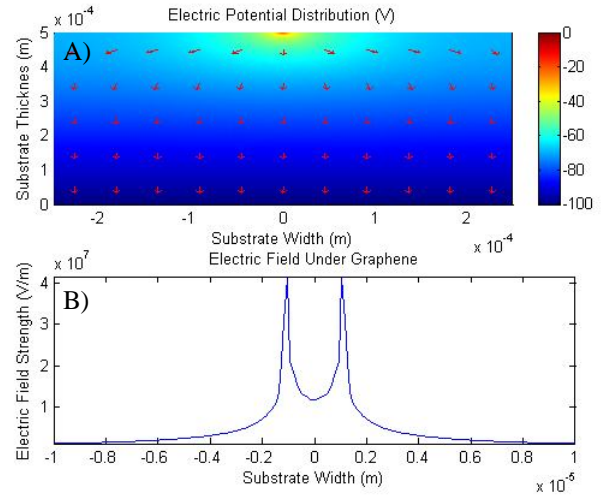


Fig. 5. A) COMSOL simulation of the field lines created with a gate voltage of $V_G = -100$ V, applied from the electrode on the bottom of the absorber to the graphene (taken to be 2 μ m wide in this simulation). The field lines, shown as red arrows, reveal the path of the drifted electrons (note the electron velocity is opposite to the arrow), which converge under the graphene, independent of initial position. B) The line plot shows the electric field strength 5 nm below SiO₂ near the graphene region.

In a GRD described above, the insulating buffer layer prevents the electrons from flowing into the graphene. Since the electrons build up under the insulator, the final and maximum change in electric field experienced by the graphene (after all electrons created in one radiation interaction event are drifted under the graphene), to be measured by the change of graphene resistance, is directly related to the number of electrons created. In order to “reset” the sensor and prepare it for the subsequent measurement, a smaller voltage, V_F , can be applied horizontally between the doped source and drain, which are embedded in the absorber (Fig. 6). The drift velocity in the transverse direction can be made much smaller than that in the vertical direction, allowing for all of the electrons to settle under the graphene

uniformly before they are collected through the drain. As with a GFET, a constant current flows through graphene during the operation of the detector, and the resistance of graphene is monitored.

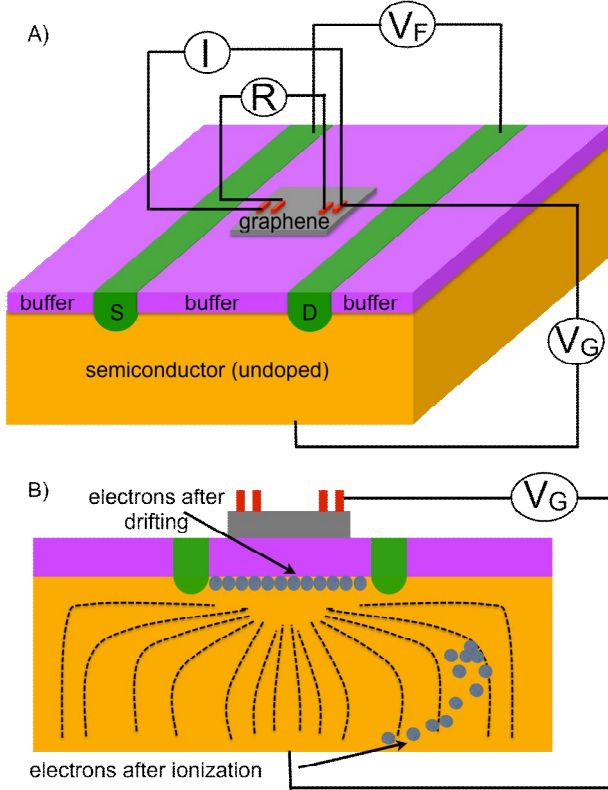


Fig. 6. In a GRD, the electrons created by the ionizing radiation in the absorber are drifted and accumulate between the absorber and the insulating buffer layer (A). The back of the absorber is coated by metal to serve as a gate electrode, while the top electrode is the graphene layer. Applying a gate voltage, V_G , field lines are produced which direct the electrons towards the graphene. Current is supplied across the graphene sample, and the resistance of the graphene layer is monitored. With the electrons accumulated under the insulator layer, the electric field change measured through the graphene resistance, is directly related to the number of electrons created by the radiation event. A voltage, V_F , between the source and drain within the absorber slowly drifts the electrons horizontally preventing electron pile-up. V_F is much smaller than the gate voltage, V_G , in order to acquire the signal before the electrons drain. (B) shows a cross section of a GRD showing electrons both before and after they are drifted. The path the electrons take is determined from the electric field lines, which are signified by the dotted lines.

B. Energy Resolution

Energy resolution is the key performance parameter when considering the use of the proposed architectures for SNM detection. Contributions to the finite energy resolution of the GRDs include both the intrinsic (Poissonian) fluctuation of the number of charge carriers produced for a given deposited energy, and the limitations of the detector architecture, including the effects such as charge trapping [10], loss of charge to auxiliary electrodes, and inaccuracies in the measurement of graphene resistance.

Here we succinctly discuss the needed resistance measurement accuracy and the maximum lateral drift velocity which will not compromise the detector resolution, i.e. which allows the resolution associated with the Poissonian

distribution of the number of charge carriers in the substrate to be achieved. For this discussion a 1-MeV energy-depositing event is assumed in a Si substrate, resulting on average in production of $N=2.73 \times 10^5$ electron-hole pairs. The $1-\sigma$ fluctuation in the number of electron-hole pairs produced is 522.7, or 0.19% ($\sim 1/\sqrt{N}$), which is the theoretical maximum resolution achievable with this substrate at this energy.

C. Resistance Measurement Accuracy

To estimate the required accuracy for measurement of graphene resistance, the electric field generated by the accumulated electrons is calculated first. The electric field is calculated using

$$E = \frac{Q}{2 \epsilon A}, \quad (4)$$

where E is the electric field, Q is the charge, A is the area of the graphene, and ϵ is the permittivity. The factor of $1/2$ is the result of the graphene only being on the one side of the accumulated electrons. Using a relative permittivity of 4 for SiO_2 and an area of $10 \mu\text{m}^2$, the expected electric field is calculated to be $\sim 6 \times 10^7$ V/m. For the resistance measurement not to compromise the overall energy resolution, the accuracy of the electric field measurement is assumed to be 0.1% of the electric field. Using the up-slope of the resistance curve measured in a typical GFET device (Fig. 1), this is equivalent to a change in resistance of $\sim 10 \Omega$, which can be resolved with common electronics. For the current highest achievable field effect slope near Dirac point [9] this results in a resistance change of $\sim 100 \Omega$.

D. Lateral Drift Velocity for Draining the Charges

A continuous lateral drift can be applied to drain the ionized charges (accumulated at absorber-buffer interface) following the single-event measurement to prepare the detector for the subsequent measurement. The choice of lateral drift speed is a trade-off between the detector speed (higher lateral electric field applied), and the need to make an accurate measurement of the resistance change in graphene prior to charges being drifted away from the sensitive region directly below graphene. We assume that a loss of 0.1% of the total charge produced by ionization due to lateral drift prior to resistance measurement will result in a negligible loss of resolution. This means the drift time through the absorber needs to be shorter than 0.1% of the drift time to the drain. The drift speed can be calculated from

$$\tau_d = \frac{d^2}{\mu |V|}, \quad (5)$$

where τ_d is the drift time through the absorber, μ is the electron mobility, d is the distance traveled, and V is the potential. For an absorber thickness of 0.5 mm, a potential of -100 V, and a uniform mobility of $1250 \text{ cm}^2/(\text{V s})$, the drift

time is calculated to be 20 ns. From this, we calculate that the minimum lateral drift time needs to be 20 μ s. If the distance between the absorber source and drain is \sim 6 μ m (double the graphene width), the voltage across the absorber source and grain (“S” and “D” in Fig. 6) needs to be \sim 16 μ V. While small, setting this voltage is still possible with commercial electronics. For this lateral drift time, the detection rate limit based on the detector design is set at 50 kHz.

V. DISCUSSION AND CONCLUSIONS

Graphene-based sensors have a potential to provide a novel, unique mechanism for detection of ionizing radiation. The sharp transition in resistance as a function of electric field allows the graphene to act as a built-in preamplifier. We can also view the GRD as an (indirect) photoconductor with high gain of transconductance due to the sharp field effect of graphene.

In addition, the proposed GRD utilizes the unique material properties of graphene to provide several potential operational advantages over conventional MOSFET (which could also be utilized as radiation sensors). Graphene has low electrical noise which could otherwise limit the sensitivity of conventional detectors [6]. Graphene’s high electrical conductivity and pristine crystallographic nature allow for the reduction of Johnson and Pink (1/f) noise [6,11] from degrading acquired signals. Noise immunity is retained throughout graphene’s conductivity range, including Dirac point, where resistivity is at a maximum (but finite, while a conventional MOSFET resistance would diverge when depleted), as well as during ambipolar operation in n-type or p-type modes [1].

A performance gain in operation speed is also expected with GRD. Dual gated GFETs have been shown to produce cutoff frequencies as high as 50 GHz, or much higher than the cutoff frequency obtainable in Si MOSFET designs of comparable size [12]. Graphene can be deposited or transferred on a number of substrates expanding the library of compatible absorber materials for GRD development. This allows for the incorporation of narrow bandgap semiconductors in the device architecture which could improve the energy resolution with less stringent requirement on the substrate purity or carrier mobility and lifetime. A narrow bandgap semiconductor such as indium antimonide (InSb) is a candidate for implementation in a GRD and could provide an increase in energy resolution when compared to current Ge-based detectors.

We have created a proof of concept model for detecting radiation using a GFET, and also conducted a preliminary design for a graphene-based detection scheme capable of providing energy resolution, simultaneously allowing for a large scale detector to be operated while using a much smaller size graphene layer. GFET has a number of potential advantages resulting from the unique properties of graphene,

including high speed [12] and low noise (even at room temperature) [6]. Various absorber material (including narrow bandgap semiconductors) may be used to optimize the electrical properties and energy resolution in this novel detector.

ACKNOWLEDGMENTS

This research was performed under the project “Graphene-based ultrasensitive advanced radiation detectors” (GUARD), an “Academic Research Initiative” (ARI) program supported by U.S. National Science Foundation Directorate of Engineering and U.S. Department of Homeland Security’s Domestic Nuclear Detection Office. YPC also acknowledges the support of the Defense Threat Reduction Agency (DTRA) Young Investigator Program. A portion of M. Foxe’s research was performed under the Nuclear Forensics Graduate Fellowship Program which is sponsored by the U.S. Department of Homeland Security’s Domestic Nuclear Detection Office and the U.S. Department of Defense’s Defense Threat Reduction Agency. We also acknowledge helpful discussions with Prof. Serge Luryi and Dr. Ionel Hau.

REFERENCES

- [1] A.K. Geim and K.S. Novoselov., “The Rise of Graphene”. *Nature Materials*, vol. 6, no. 3, pp. 183-191, March 2007.
- [2] K.S. Novoselov, *et al.* “Electric field effect in atomically thin carbon films”. *Science* vol. 306, pp. 666-669, 2004.
- [3] S. A. Pozzi, E. Padovani, and M. Marseguerra, “MCNP-PoliMi: A Monte Carlo Code for Correlation Measurements,” *Nucl. Instrum. Methods A*, vol. 513, no.3, pp. 550-558, Nov. 2003.
- [4] P. Hovington *et al.*, *Scanning*, vol. 19, no. 1, pp. 1-14, Jan, 1997
- [5] COMSOL Multiphysics, <http://www.comsol.com>.
- [6] F. Schedin *et al.*, “Detection of individual gas molecules adsorbed on graphene”, *Nature Materials*, vol. 6, no. 9, pp. 652-655, Sep.2007.
- [7] S. Friedrich, “Nuclear Diagnostics with Cryogenic Spectrometers,” in *11th Symposium on Radiation Measurements and Applications*, Ann Arbor, MI, 2006, pp. 157-160.
- [8] N. Tsoulfanidis, “Measurement and Detection of Radiation”, 1986, pp. 249.
- [9] K. I. Bolotin *et al.*, “Ultrahigh electron mobility in suspended graphene”, *Solid State Communications* Vol. 146, pp. 351-355, Mar. 2008.
- [10] Z. He, G.F. Knoll, D.K. Wehe, and J. Miyamoto, “Position-sensitive single carrier CdZnTe detectors,” *Nucl. Instrum. Methods A* vol. 388, no. 102, pp. 180-185, Mar. 1997
- [11] Y-M. Lin and P. Avouris, “Strong Suppression of Electrical Noise in Bilayer Graphene Nanodevices”, *Nano Lett.*, Vol. 8, pp 2119-2125, 2009
- [12] Y-M. Lin *et al.*, “Dual-Gate Graphene FETs With f_T of 50 GHz”, *IEEE EDL*, vol. 31, pp 68-70, Jan. 2010.